

Molecular Profiling and Classification of Sporadic Renal Cell Carcinoma by Quantitative Methylation Analysis

Mark L. Gonzalgo,
Srinivasan Yegnasubramanian, Gai Yan,
Craig G. Rogers, Theresa L. Nicol,
William G. Nelson, and Christian P. Pavlovich

The James Buchanan Brady Urological Institute, The Johns Hopkins Medical Institutions, Baltimore, Maryland

ABSTRACT

Purpose: Preoperative histologic classification of solid renal masses remains limited with current technology. We determine the utility of molecular profiling based on quantitative methylation analysis for characterization of sporadic renal cell carcinoma.

Experimental Design: Primary renal cell carcinomas representing three different histologic subtypes were obtained from a total of 38 patients who underwent radical nephrectomy for suspected malignant disease. Genomic DNA was isolated from tumors and was subjected to sodium bisulfite modification. The normalized index of methylation (NIM) for each sample was determined by quantitative real-time methylation-specific PCR at 17 different gene promoters. Hierarchical cluster analysis was performed by using an unsupervised neural network with binary tree topology.

Results: The majority of gene promoters that were analyzed in this study demonstrated very low levels of methylation (NIM <1.0). The *RASSF1A* gene promoter, however, was methylated in 30 of 38 (79%) cases. The frequency of *RASSF1A* methylation in papillary, clear-cell, and oncocytoma subtypes was 100, 90, and 25%, respectively. The highest levels of *RASSF1A* methylation were observed in the papillary (mean NIM = 78.9) and clear-cell (mean NIM = 13.4) subtypes. The vast majority of oncocytomas were completely unmethylated, and none demonstrated >1% methylation (mean NIM = 0.11). Hierarchical cluster analysis based on quantitative methylation levels resulted in stratification of sporadic renal cell carcinomas into their discrete histologic subtypes.

Conclusions: Classification of sporadic renal cell carcinomas into histologic subtypes can be accomplished via multigene quantitative methylation profiling. Validation of

this approach and selection of appropriate methylation markers may ultimately lead to use of this technology in the preoperative assessment of suspicious renal masses.

INTRODUCTION

It is estimated that 35,710 new cases of renal cancer will be diagnosed and 12,480 people will die of the disease in the year 2004 (1). Renal cell carcinoma (RCC) consists of a heterogeneous group of epithelial tumors that range in biological potential from entirely benign to aggressively malignant (2, 3). Clear-cell carcinoma is the most common subtype of RCC, accounting for 70 to 80% of all renal epithelial tumors (4). Papillary carcinoma is the second most frequent RCC variant and comprises approximately 10 to 15% of renal tumors. Renal oncocytomas are considered benign and are next most common in prevalence, accounting for 3 to 7% of renal tumors (5). At the present time, relatively few preoperative predictors of malignancy or histologic subtype exist in clinical practice. Present diagnostic imaging modalities cannot always differentiate between benign and malignant solid renal masses, and, as a result, the treatment of choice for all suspicious renal masses is surgical removal. Therefore, it would be of great benefit to identify molecular markers that could distinguish benign from malignant disease.

A large number of cytogenetic alterations have been described for the different histologic RCC subtypes, which have, in turn, allowed for modern classification systems for renal epithelial tumors (2, 6, 7). Clear-cell RCC is characterized by *VHL* (3p25) mutations and/or inactivation, chromosome 3p loss, and 5q gain (8, 9). Trisomy of chromosomes 7 and 17 is common in papillary RCC, and abnormalities of chromosomes 12, 16, 20, and Y, as well as *c-MET* mutations (7q31) are also occasionally found in such tumors (6, 10). Loss of chromosomes 1 and Y, loss of heterozygosity at 14q, and abnormalities involving 11q13 have been reported for oncocytomas, although many oncocytomas have no obvious cytogenetic abnormalities (6, 11). Modern RCC classification systems take into account cytogenetic, molecular genetic, and histologic differences between RCC tumor subtypes and have been validated by these findings.

A molecular marker that has only recently been investigated in renal cancers is aberrant DNA methylation. Methylation at cytosines located at CpG dinucleotides is a ubiquitous but regulated phenomenon essential for normal mammalian development (12). Hypermethylation of CpG islands in the promoter regions of genes is associated with transcriptional silencing and is a frequent event in human cancer (13). We sought to determine the methylation profiles of 38 sporadic renal cancers at 17 gene loci and assess the utility of quantitative multigene DNA methylation analysis for stratification of RCC subtypes.

Received 12/6/03; revised 6/23/04; accepted 7/20/04.

The costs of publication of this article were defrayed in part by the payment of page charges. This article must therefore be hereby marked *advertisement* in accordance with 18 U.S.C. Section 1734 solely to indicate this fact.

Requests for reprints: Mark Gonzalgo, Sidney Kimmel Comprehensive Cancer Center, 1650 Orleans Street, CRB 151, Baltimore, MD 21231-1000. Phone: (410) 614-3252; Fax: (410) 502-9817; E-mail: mgonzal@jhmi.edu.

©2004 American Association for Cancer Research.

MATERIALS AND METHODS

Patients and Specimen Collection. A total of 38 patients who were treated with radical or partial nephrectomy for suspected renal malignancy were selected for this study. All of the patients provided informed consent for use of tissues, and this protocol was approved by The Johns Hopkins University School of Medicine Institutional Review Board (IRB). Normal kidney tissue was obtained from nephrectomy specimens at a location that was distant from the area of tumor involvement. Normal and tumor kidney tissues were snap-frozen and stored at -70°C before analysis.

DNA Isolation, Bisulfite Modification, and Real-time Methylation-Specific PCR. Total DNA was extracted from kidney tissues and 1 μg was subjected to sodium bisulfite modification with the CpGenome DNA Modification kit (Serologicals Co., Norcross, GA). Real-time methylation-specific PCR (RT-MSP) was performed with a technique based on principles of the MethyLight assay (14). Bisulfite-modified DNA was amplified with real-time PCR with primers and probes complementary to a region of the *MYOD1* promoter that did not contain any CpG dinucleotides but did contain non-CpG cytosines, to ascertain the amount of converted templates in each sample. DNA methylation patterns in the promoters of the 17 genes included in this study were then assayed by real-time PCR amplification of bisulfite-modified DNA with primers and Taqman probes specific for fully methylated bisulfite-converted sequences.

The primer and probe sequences used for this study are listed in Table 1. All PCR reactions were carried out on an iCycler real-time thermal cycler (Bio-Rad, Hercules, CA) at 95°C for 8.5 minutes followed by 45 cycles of 95°C for 15 seconds, 60°C for 30 seconds, and 72°C for 30 seconds. The *EDNRB* reaction was carried out under the same conditions, except that an annealing temperature of 64.5°C was used. Each PCR reaction was carried out in a 25- μL volume containing 2.5

μL of $10\times$ PCR buffer; 1 unit of AmpliTaq Gold (Applied Biosystems, Foster City, CA); 2.5 mmol/L forward primer; 2.5 mmol/L reverse primer; 200 nmol/L Taqman probe; 0.25 mmol/L concentration of dATP, dCTP, dTTP, and dGTP; 5.5 mmol/L MgCl_2 ; and 1 μL template DNA. Bisulfite-converted *Sssl*-treated white blood cell DNA served as a positive control and was used to generate a standard curve to quantify the amount of fully methylated alleles in each reaction. Bisulfite-converted white blood cell DNA from normal volunteers and blank reactions with water substituted for DNA served as negative controls. All PCR reactions for each locus and sample examined were performed in triplicate, and the mean quantitative methylation level was recorded. The normalized index of methylation (NIM) was defined as the ratio of the amount of methylated templates at the promoter of interest to the amount of converted *MYOD1* templates in any given sample. The NIM serves as an index of the percentage of input copies of DNA that are fully methylated at the primer- and probe-binding sites.

Bisulfite Genomic Sequencing of the *RASSF1A* Gene. Bisulfite genomic sequencing of *RASSF1A* was performed as described previously (15, 16). Briefly, 25 ng of bisulfite-converted DNA was mixed with 2.5 μL of $10\times$ PCR Buffer II, 1.25 units AmpliTaq Gold, 0.5 $\mu\text{mol/L}$ primers (forward: 5'-GTTTTYGTAGTTAATGAGTTTAGGTTTTTTT-3', reverse: 5'-ACCCCTCTCCTCTAACACAATAAACTAACC-3'), 200 $\mu\text{mol/L}$ concentration of each dNTP, and 5 mmol/L MgCl_2 in a total reaction volume of 25 μL . PCR amplification was carried out at 95°C for 10 minutes, followed by 25 cycles of 95°C for 15 seconds, 55°C for 15 seconds, and 74°C for 30 seconds, and ended with a 6-minute extension at 74°C . PCR products were purified with the QIAquick PCR Purification kit (Qiagen, Valencia, CA). Approximately 1 to 2 μL of the purified DNA solution was amplified in a semi-nested PCR under similar conditions for 30 cycles, with each cycle consisting of 95°C for 30 seconds, 55°C for 30 seconds, and 74°C for 1 minute. The

Table 1 Primers and Taqman probes used for all loci in this study

HUGO gene name	5' to 3' forward primer	5' to 3' Taqman probe	5' to 3' reverse primer
<i>RASSF1A</i>	GCGTTGAAGTCGGGGTTC	6FAM-ACAAACCGGAACCGAACGAAACCA-BHQ1	CCCGTACTTCGCTAACTTTAAACG
<i>CDH1</i>	AATTTTAGGTTAGAGGGTTATCGCGT	6FAM-CGCCACCCGACCTCGCAT-BHQ1	TCCCAAAAACGAAACTAACGAC
<i>MLH1</i>	CTATCGCCGCTCATCGT	6FAM-CGCGACGTCAAACGCCACTACG-BHQ1	CGTTATATATCGTTTCGTAGTATTCGTGTTT
<i>BHD</i>	CGTTATTTTCGGGTGATATTTTGTGCG	6FAM-GGTGTGATTCCGCCGGTCCGGGT-BHQ1	AAACTCGACAACCGAAATCCCG
<i>VHL</i>	TGGAGGATTTTTTGTGCTACGCG	6FAM-CGCTCCCGAATCGACCTCCGTAATCTT-BHQ1	CGAACCGAACGCCGCGGAA
<i>INK4a/ARF</i>	ACGGGCGTTTTTCGGTAGTT	6FAM-CGACTCTAAACCTACGCACGCGAAA-BHQ1	CCGAACCTCCAAAATCTCGA
<i>PTGS2</i>	CGGAAGCGTTCGGGTAAG	6FAM-TTTCGGCAAATATCTTTCTCTTCGCA-BHQ1	AATTCACCCGCCAAAAC
<i>EDNRB</i>	GGTTACGCGGGGAAGAAAATAGTTG	6FAM-CATAACTCGCAACGCGAATCGAACTCC-BHQ1	ATACCGCCCGCAACCTCTTCG
<i>MDR1</i>	GGCGGGTAAAGTTTGAACGCG	6FAM-CCTATACGCGAAATCTCCAACATCTCCACG-BHQ1	AAACGCCCGCGTTAATACCCCA
<i>TIMP3</i>	GCGTCGGAGTTAAGGTTGTT	6FAM-AACTCGTCCGCCCGGAA-BHQ1	CTCTCCAAAATTACCGTACGCG
<i>CDKN2a</i>	TGGAGTTTTTCGGTTGATTGGTT	6FAM-ACCCGACCCCGAACCCG-BHQ1	ACAACGCCCGCACCTCTCT
<i>CDKN2B</i>	AGGAAGGAGAGAGTGCCTCG	6FAM-TTAACGACACTCTTCCCTCTTCCACG-BHQ1	CGAATAATCCACCGTTAAACCG
<i>APC</i>	TTATATGTCGGTACGTGCGTTTATAT	6FAM-CCGTCGAAAACCCGCCGATTA-BHQ1	GAACCAAAAACGCTCCCAT
<i>GSTP1</i>	AGTTGCGCGCGGATTTTC	6FAM-CGGTCGACGTTCCGGGTGTAGCG-BHQ1	GCCTCCAACTAAATCAGGACG
<i>MGMT</i>	GCGTTTCGACGTTTCGTAGTT	6FAM-CGAAACGATACGCACCCGCA-BHQ1	CACCTTCCGAAAACGAAACG
<i>DAPK</i>	GGATAGTCGGATCGAGTTAACGTC	6FAM-ACCCTACCGCTACGAAATACCGAATCCCT-BHQ1	CCCTCCCAACGCCGA
<i>ESR1</i>	GGCGTTCGTTTTGGGATTG	6FAM-CGATAAAAACCGAACCCGACGA-BHQ1	GCCGACACGCGAACTCTAA
<i>MYOD1</i>	CCAACTCCAAATCCCTCTCTAT	6FAM-TCCTTCTATTCTAAATCCAACTAAATACCTCC-BHQ1	TGATTAATTTAGATTGGGTTTAGAGAAGGA

NOTE. Sequences listed are specific for sodium bisulfite-converted DNA. Primers and probes for the *MYOD1* locus do not contain any CpG dinucleotides, making this primer set insensitive to methylation and appropriate as a conversion control.

Abbreviations: HUGO, Human Genome Organization nomenclature; 6FAM, 6-carboxyfluorescein; BHQ1, 3' quencher.

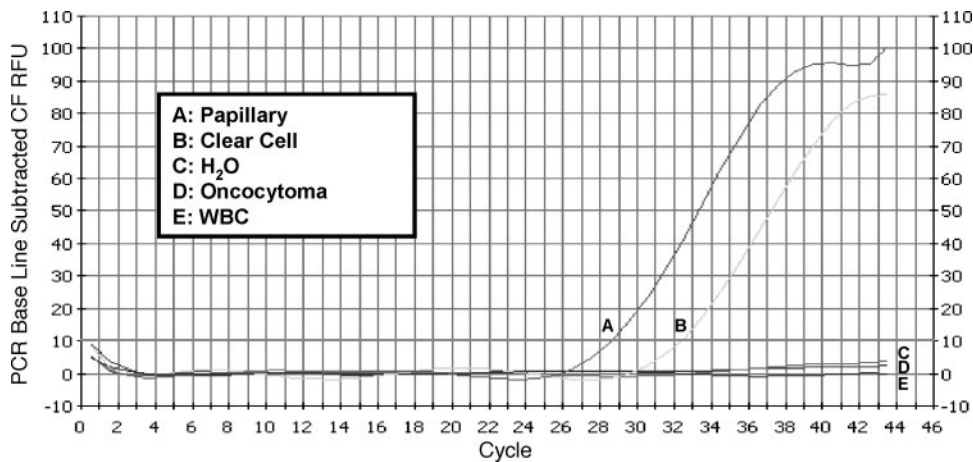


Fig. 1 Real-time quantitative PCR amplification plots of *RASSF1A* gene methylation in RCC. Three kidney tumor subtypes including controls are shown: A, papillary; B, clear-cell; C, water blank (H_2O); D, oncocytoma; E, white blood cell DNA (WBC). (CF-RFU, curve fit relative fluorescence units.)

inner primer set sequences were 5'-TAATGAGTTTAGGT-TTTTTYGATATGGT-3' (forward) and 5'-AACACAATAA-AACTAACCTCCAAAAAC-3' (reverse). PCR products were gel-purified (QIAquick Gel Extraction kit, Qiagen), then cloned into the pCR4-TOPO vector (TOPO TA Cloning kit, Invitrogen, Carlsbad, CA). After transformation, 10 colonies per specimen were expanded overnight and plasmid DNA was extracted (QIAprep Spin Miniprep kit, Qiagen). Sequencing was performed by the DNA Analysis Facility at the Johns Hopkins University Medical Institution (Baltimore, MD).

Hierarchical Clustering of Sporadic Renal Cell Carcinoma According to CpG Island Promoter Hypermethylation. Cluster analysis was performed in a blinded manner with the self-organizing hierarchical neural network SOTA (self-organizing tree algorithm), an unsupervised neural network with a binary tree topology (17). An unrestricted growth algorithm was used to generate a dendrogram for classification of tumor subtypes based on data obtained from quantitative real-time PCR analyses. The TREEVIEW program was used to visualize the out file as a binary tree (19). Matrix values were transformed into a graded color pattern representing the level of methylation for each point of the matrix (see Fig. 1). Application of hierarchical clustering algorithms to methylation data has been previously validated (18, 19).

Statistical Analysis. The mean NIM and exact binomial 95% confidence intervals were calculated for each gene locus and tumor type. The association between *RASSF1A* promoter methylation and clinical/pathologic characteristics was examined with two-sided, Fisher's exact test. All analyses were performed with STATA 7.0 (Stata Corporation, College Station, TX).

RESULTS

We analyzed DNA obtained from nephrectomy specimens of 38 patients for the presence of gene methylation. Distinct CpG islands associated with 17 gene promoters were examined (see Table 1). The loci were chosen based on their established relevance to various human cancers and, specifically, renal cell carcinoma, as reported in the literature (20–24). The clinical and pathologic characteristics of our study group are shown in Table

2. Sufficient DNA was obtained from all 38 tumor specimens to generate PCR products after sodium bisulfite modification.

Methylation analysis was performed with fluorescence-based, RT-MSP (14). Results from a typical PCR analysis of renal tumors at one gene locus (*RASSF1A*) are shown in Fig. 1. Papillary tumors frequently demonstrated higher levels of *RASSF1A* methylation compared with clear-cell carcinomas or oncocytomas as indicated by a lower threshold cycle. Each primer pair and corresponding probe was designed to evaluate the methylation status of 6 to 11 CpG dinucleotides for each gene promoter that was examined. On average, 9 CpG dinucleotides were sampled by each primer and probe set. Hybridization of primers and probes is contingent on the presence of a high degree of methylation at CpG sites in the region of oligonucleotide hybridization. Thus, the primer and probe sets were designed for the highest level of methylation specificity. Possible explanations for a negative result include: partial methylation, no methylation, or absence of the region of interest area (*i.e.*, homozygous deletion).

Hierarchical Clustering of Renal Tumors on the Basis of DNA Methylation. Results from RT-MSP analysis of 38 renal tumors (21 clear-cell RCC, 9 papillary RCC, and 8 oncocytomas) are shown in Fig. 2A. The NIM color scale ranges

Table 2 Clinical and pathologic characteristics of patients undergoing nephrectomy

No. of patients	38
Males, <i>N</i> (%)	28 (73.7)
Females, <i>N</i> (%)	10 (26.3)
Mean, age \pm SD	61.1 \pm 13.3
Tumor size, <i>N</i> (%)	
<4.0 cm	13 (34.2)
\geq 4.0 cm	25 (65.8)
Pathologic stage, <i>N</i> (%)	
T1	19 (50.0)
T2	10 (26.3)
\geq T3	9 (23.7)
Furhman grade, <i>N</i> (%)	
I-II	23 (60.5)
> II	15 (39.5)

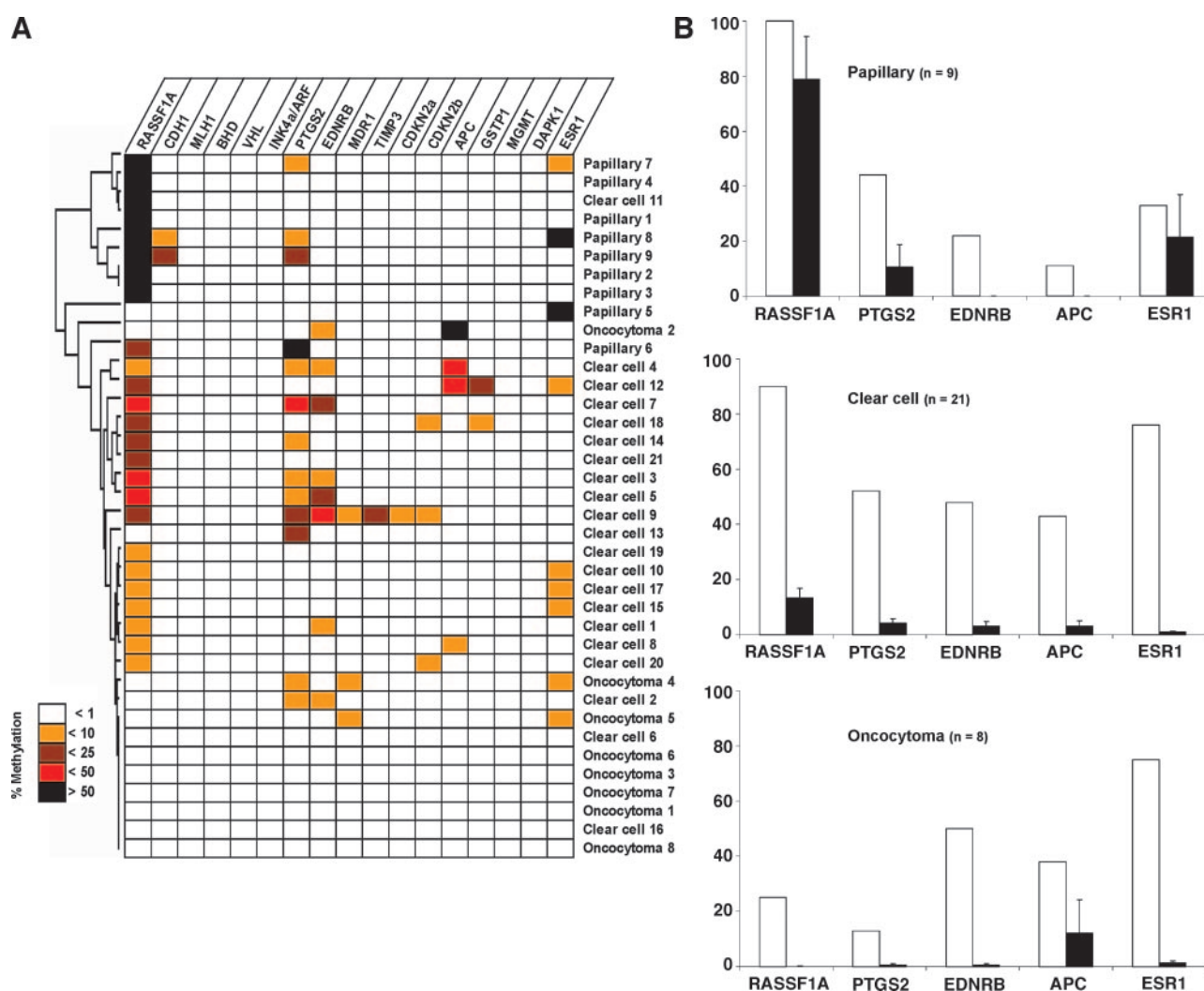


Fig. 2 Methylation profile of sporadic RCCs. *A*, at left, dendrogram generated from hierarchical cluster analysis; color scale at the bottom left, methylation levels; at the top of the figure, the 17 genes analyzed for methylation; on the right side of the matrix, histologic tumor subtype, clustered based on hierarchical analysis. *B*, frequency and mean NIM of certain genes stratified according to RCC subtype; white columns, frequency of methylation (%); black columns, mean NIM for each gene.

from white (<1% methylation) to black (>50% methylation) for each sample analyzed. Cluster analysis based on NIM values for each gene and tumor was performed in a blinded manner with a self-organizing tree algorithm (17). The dendrogram generated from an unrestricted growth algorithm for classification of tumor subtypes is shown to the left of Fig. 2A. The remarkable finding of this experiment was that CpG island hypermethylation alone allowed for classification of most of the renal tumors according to their histologic subtype. A total of 7 (78%) of 9 papillary RCCs clustered into an independent primary branch from the other histologic subtypes of renal tumors. A total of 20 (91%) of 21 clear-cell RCCs and 8 (100%) of 8 oncocytomas shared the same primary branch that was separate from papillary RCCs. An additional distinction between clear-cell RCCs and oncocytomas was observed; 6 (75%) of 8 oncocytomas clustered into an independent terminal branch. Although it is apparent that the clustering algorithm was

predominantly influenced by the degree of *RASSF1A* methylation, our findings represent the first evidence that DNA methylation can potentially be used as a molecular marker for the stratification of renal tumors into discrete histologic subtypes.

Frequency and Level of Gene Hypermethylation in Renal Tumors. High levels of *RASSF1A* promoter methylation were frequently detected in papillary and clear-cell RCCs compared with oncocytomas (see Figs. 1 and 2). Methylation of *RASSF1A* was detected in a total of 9 (100%) of 9 papillary RCCs and 19 (90%) of 21 clear-cell RCCs. The mean NIM was 78.9 [95% confidence interval (CI), 43.1–114.7] for papillary RCCs and 13.4 (95% CI, 6.2–20.6) for clear-cell RCCs. In contrast, no significant methylation of *RASSF1A* was detected in the eight oncocytomas that were examined. Two oncocytomas had extremely low levels of methylation (<1%) as demonstrated by the mean NIM value of 0.11, which was ~720-fold and 120-fold lower than papillary and clear-cell RCCs, respec-

tively. Other genes were frequently methylated in renal tumors, albeit at low levels, and included: *PTGS2*, *EDNRB*, *APC*, and *ESR1*. The frequency and mean NIM for each of these genes stratified according to histologic subtype is shown in Fig. 2B.

Frequency and Level of Gene Hypermethylation in Normal Kidney and Renal Tumor Pairs. Results from RT-MSP analysis of *RASSF1A*, *PTGS2*, *EDNRB*, *APC*, and *VHL* among 22 normal kidney and tumor pairs (6 papillary RCCs, 14 clear-cell RCCs, and 2 oncocytomas) are shown in Fig. 3A. Interestingly, we found that neighboring normal kidney tissue was frequently methylated at low levels in some genes. A total of 20 (91%) of 22 normal renal tissue specimens had detectable *RASSF1A* methylation. Fig. 3B shows the frequency and mean NIM for normal kidney, papillary RCC, clear-cell RCC, and

oncocytoma, stratified according to certain genes that were studied (*RASSF1A*, *PTGS2*, *EDNRB*, and *APC*). The mean NIM level of *RASSF1A* in normal kidney was 13.5 (95% CI: 9.5–17.5). The frequency and mean NIM of *RASSF1A* in the corresponding paired papillary RCCs, clear-cell RCCs, and oncocytomas was 100% (mean NIM = 60.8), 86% (mean NIM = 12.8), and 50% (mean NIM = 0.09), respectively.

Bisulfite Genomic Sequencing of the *RASSF1A* Gene Locus. We performed bisulfite genomic sequencing of the *RASSF1A* gene locus to determine the exact nature of methylation patterns that existed in all three tumor subtypes and normal kidney (see Fig. 4). Papillary tumors demonstrated higher levels of methylation compared with clear-cell tumors or oncocytomas. There was an excellent correlation between results ob-

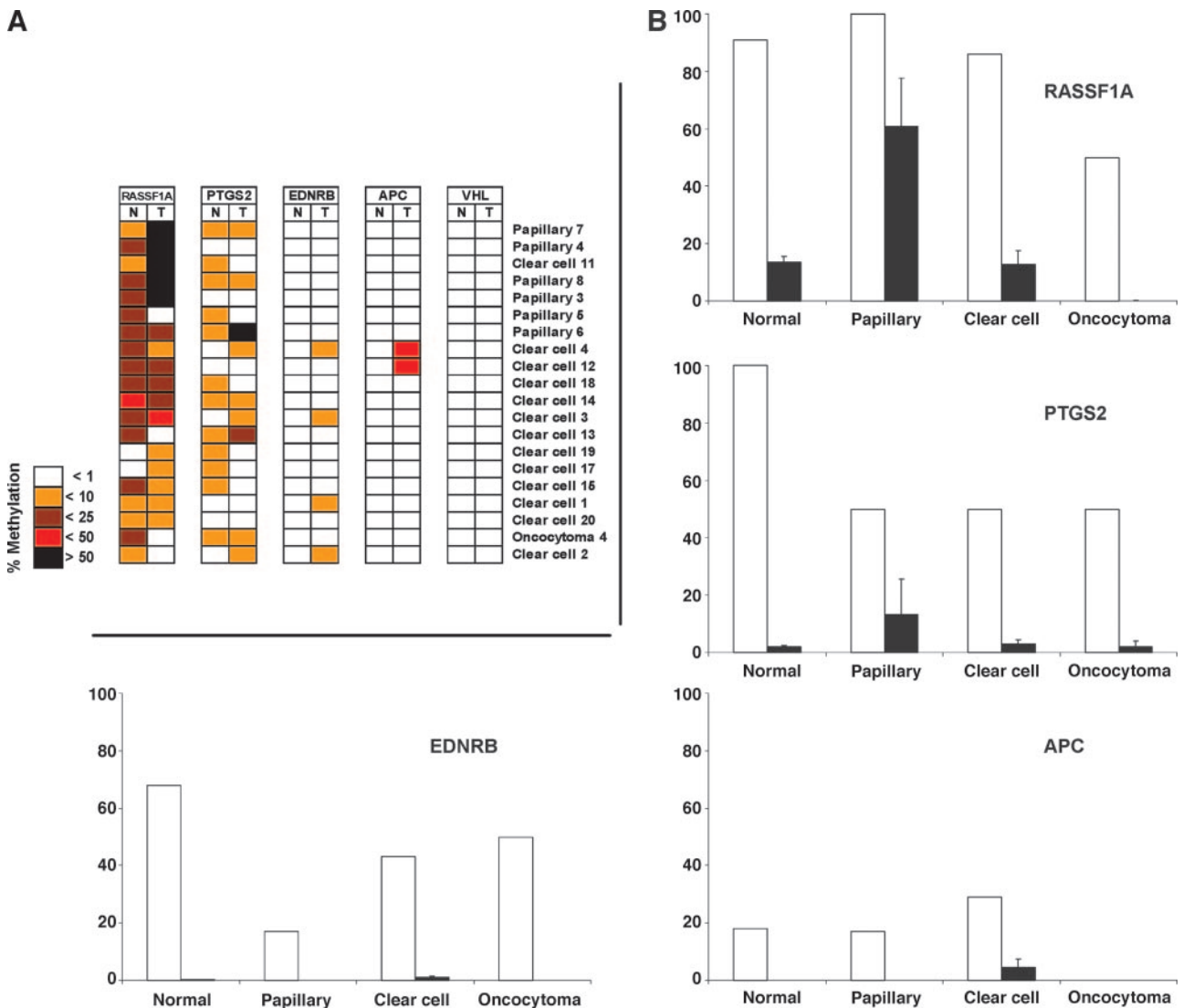


Fig. 3 Methylation profile of normal and tumor kidney pairs. A, methylation profiles of 5 genes; color scale at the bottom left, methylation levels; on the right side of the matrix, histologic tumor subtype, clustered based on hierarchical analysis; N, normal; T, tumor. B, frequency and mean NIM for normal kidney, papillary RCC, clear-cell RCC, and oncocytoma, stratified according to gene locus; white columns, frequency of gene methylation (%); black columns, mean NIM for each gene.

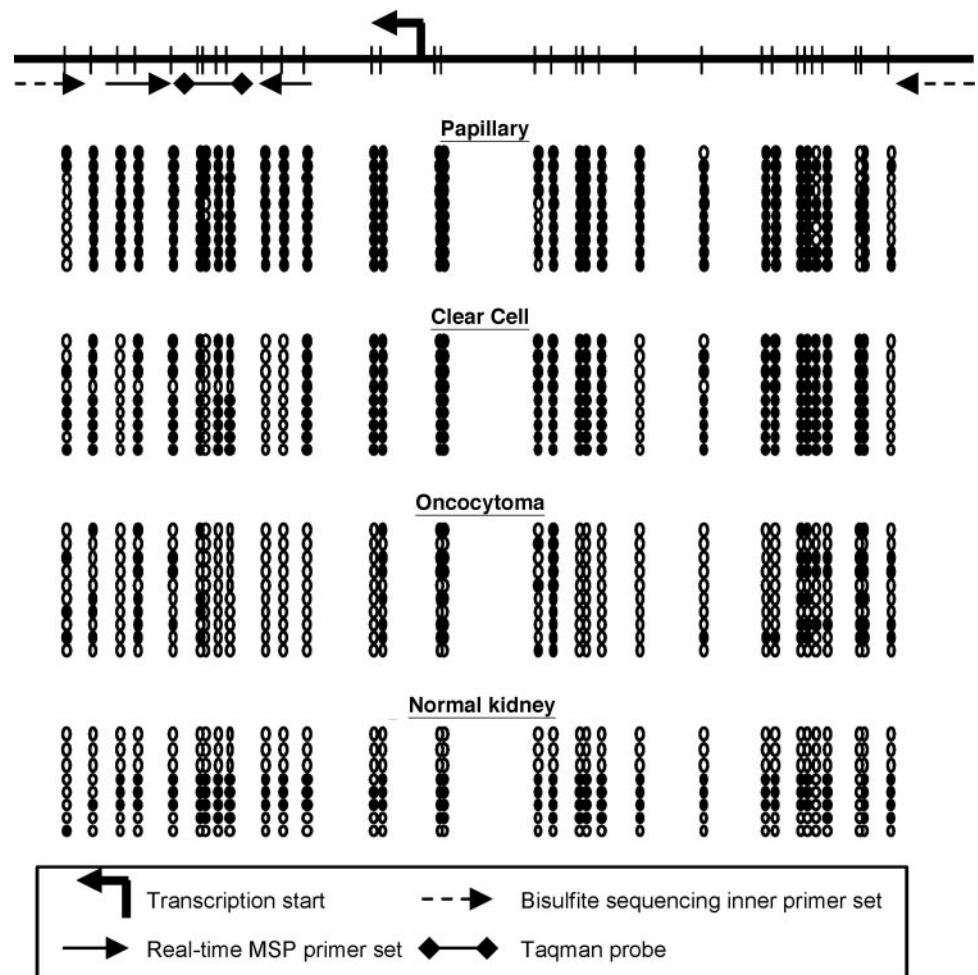


Fig. 4 Bisulfite genomic sequencing of *RASSF1A* gene methylation in RCC; results from methylation analysis of papillary, clear-cell, oncocytoma, and normal kidney. Tick marks (top of figure), location of CpG dinucleotides; ○, unmethylated CpG; ●, methylated CpG; arrows, location of MSP primers, bisulfite sequencing primers, and Taqman probe.

tained by bisulfite sequencing and the region analyzed by RT-MSP for each tumor subtype. Bisulfite sequencing also confirmed the presence of a low degree of methylation in normal kidney as observed by the real-time quantitative PCR data and the work of others (25). These results provide further validation of the RT-MSP methodology used in our experiments and previously published work (14, 18, 20, 21, 26).

Relationship between *RASSF1A* Methylation and Clinical/Pathologic Variables. We determined whether *RASSF1A* methylation was associated with certain clinical or pathologic variables (see Table 3). NIM values for each tumor were stratified into one of four groups depending on the level of *RASSF1A* methylation (0–10%, 11–25%, 26–50%, >50%). Higher levels of methylation (NIM >50%) were associated with \geq T2 pathological stage of disease ($P = 0.04$). There were no other statistically significant associations between *RASSF1A* methylation and the remaining clinical or pathologic variables analyzed (*i.e.*, age, tumor size, Fuhrman grade). Significantly more oncocytomas were found to have absent or low levels of *RASSF1A* methylation (NIM <10%) compared with papillary RCCs ($P < 0.001$) and clear-cell RCCs ($P = 0.03$). Clear-cell RCCs were also more frequently observed to have low levels of methylation (NIM <10%) compared with papillary tumors ($P = 0.04$). More

papillary RCCs had higher levels of *RASSF1A* methylation (>50%) compared with clear-cell RCCs ($P < 0.001$) and oncocytomas ($P = 0.002$). These findings underscore the differences in *RASSF1A* methylation between tumor subtypes and support our data generated from hierarchical cluster analysis.

DISCUSSION

We have demonstrated for the first time that quantitative gene methylation profiling can be used to stratify RCCs into distinct histologic subtypes. The dendrogram generated from hierarchical cluster analysis (see Fig. 2A) indicates that papillary RCCs have significantly different patterns of gene methylation compared with clear-cell RCCs and oncocytomas. Although clear-cell RCCs appeared to be more closely related to oncocytomas than to papillary RCCs, 75% of oncocytomas clustered into an independent terminal branch. Furthermore, statistical analyses examining the relationship between *RASSF1A* methylation and renal tumors demonstrated concordant results with respect to the relatedness of the three histologic subtypes (see Table 3). Papillary RCCs were more frequently observed to have higher levels of *RASSF1A* methylation (>50%) compared with oncocytomas ($P = 0.002$) and clear-cell RCCs ($P <$

Table 3 Relationship between *RASSF1A* promoter methylation detected in renal tumors and clinical/pathologic characteristics

Clinical/pathologic characteristic	Methylation 0–10%	<i>P</i> *	Methylation 11–25%	<i>P</i> *	Methylation 26–50%	<i>P</i> *	Methylation >50%	<i>P</i> *
Age								
<60 (<i>N</i> = 17)	11 (65)		1 (6)		1 (6)		4 (24)	
≥60 (<i>N</i> = 21)	10 (48)	0.34	5 (24)	0.20	2 (10)	0.100	4 (19)	1.00
Tumor size								
<4 cm (<i>N</i> = 13)	10 (77)		1 (8)		1 (8)		1 (8)	
≥4 cm (<i>N</i> = 25)	11 (44)	0.09	5 (25)	0.64	2 (8)	1.00	7 (28)	0.22
Pathologic stage								
T1 (<i>N</i> = 19)	13 (68)		3 (16)		2 (11)		1 (5)	
≥T2 (<i>N</i> = 19)	8 (42)	0.19	3 (16)	1.00	1 (5)	1.00	7 (37)	0.04
Fuhrman grade								
I–II (<i>N</i> = 22)	13 (59)		1 (5)		2 (9)		6 (27)	
>II (<i>N</i> = 16)	8 (50)	0.74	5 (31)	0.07	1 (6)	1.00	2 (13)	0.43
Tumor type								
Papillary (<i>N</i> = 9)	1 (11)		1 (11)		0 (0)		7 (78)	
Oncocytoma (<i>N</i> = 8)	8 (100)	<0.001	0 (0)	1.00	0 (0)	1.00	0 (0)	0.002
Tumor type								
Clear cell (<i>N</i> = 21)	12 (57)		5 (24)		3 (14)		1 (5)	
Oncocytoma (<i>N</i> = 8)	8 (100)	0.03	0 (0)	0.28	0 (0)	0.54	0 (0)	1.00
Tumor type								
Papillary (<i>N</i> = 9)	1 (11)		1 (11)		0 (0)		7 (78)	
Clear cell (<i>N</i> = 21)	12 (57)	0.04	5 (24)	0.65	3 (14)	0.54	1 (5)	<0.001

* Two-sided, Fisher's exact test.

0.001), indicating that distinct differences exist between these types of tumors as previously determined by hierarchical cluster analysis.

We used quantitative multigene methylation analysis for molecular profiling of sporadic renal tumors. *RASSF1A* was frequently methylated to a high degree, particularly in papillary RCCs. Many genes in our panel appeared to be frequently methylated, however, the overall levels of methylation were quite low (refer to Figs. 2B and 3B). Another interesting observation was the high frequency of low levels of gene methylation in normal kidney tissue. This finding is not entirely surprising because others have reported methylation of genes such as *RASSF1A* in normal kidney (25, 27). We found no significant levels of *VHL* methylation in any of the tissues examined. The initial study that demonstrated silencing of *VHL* by DNA methylation found 5 (19%) of 26 primary kidney tumors to be hypermethylated by Southern analysis (28). A more recent study examining 240 sporadic renal tumors found that *VHL* methylation was limited to clear-cell RCCs at a frequency of only 5% (29). The high specificity of RT-MSP assay may be another explanation as to why *VHL* methylation was not detected in any of the specimens in our study. The quantitative nature of RT-MSP avoids the possibility of generating false-positive results from amplification of extremely low amounts of methylated DNA. Many of the previous reports examining *VHL* methylation in sporadic RCC have used nonquantitative methods and may be biased toward over-reporting the frequency of *VHL* methylation because of the exponential nature of PCR amplification of low amounts of methylated sequences.

Loss of heterozygosity of chromosome 3p is perhaps the most common event in clear-cell RCCs (9, 30, 31). Transcriptional silencing of *RASSF1A* (located on chromosome 3p21.3) by DNA methylation has been reported to occur in 44% of papillary RCCs and 23 to 91% of clear-cell RCCs (27, 32). Loss

of heterozygosity in combination with methylation of the remaining normal *RASSF1A* allele may account for the “two-hits” needed for complete inactivation of this candidate tumor suppressor gene. We found a high frequency of *RASSF1A* methylation in both papillary (100%) and clear-cell (90%) RCCs (see Fig. 2). However, the mean NIM was significantly higher for papillary RCCs compared with clear-cell RCCs (78.9 versus 13.4%; see Fig. 2B). It is plausible that these findings indicate frequent bi-allelic inactivation of *RASSF1A* by DNA methylation is characteristic of papillary RCCs, whereas clear-cell RCCs may have already lost a copy of the gene and, therefore, only have one remaining allele that can become hypermethylated. Our results support the hypothesis that epigenetic inactivation of *RASSF1A* by promoter methylation represents a critical step in the pathogenesis of both papillary and clear-cell RCCs as suggested by others (32).

In conclusion, development of novel molecular methods to characterize renal tumors is of paramount importance because most renal oncocytomas cannot be differentiated from malignant RCCs based on clinical or radiographic findings. We demonstrate for the first time that molecular profiling of renal tumors by quantitative methylation analysis can be used to distinguish between histologic subtypes of RCC. The candidate tumor suppressor gene *RASSF1A* was frequently methylated in papillary and clear-cell RCCs, but not in oncocytomas. Additional studies investigating the utility of DNA methylation for disease stratification and prognostication are warranted. Validation of this approach and selection of appropriate methylation markers may ultimately lead to use of this technology in the preoperative assessment of suspicious renal masses.

REFERENCES

- Jemal A, Tiwari RC, Murray T, et al. Cancer statistics, 2004. *CA Cancer J Clin* 2004;54:8–29.

2. Kovacs G, Akhtar M, Beckwith BJ, et al. The Heidelberg classification of renal cell tumours. *J Pathol* 1997;183:131–3.
3. Moch H, Gasser T, Amin MB, Torhorst J, Sauter G, Mihatsch MJ. Prognostic utility of the recently recommended histologic classification and revised TNM staging system of renal cell carcinoma: a Swiss experience with 588 tumors. *Cancer (Phila)* 2000;89:604–14.
4. Polascik TJ, Bostwick DG, Cairns P. Molecular genetics and histopathologic features of adult distal nephron tumors. *Urology* 2002;60:941–6.
5. Dechet CB, Bostwick DG, Blute ML, Bryant SC, Zincke H. Renal oncocytoma: multifocality, bilateralism, metachronous tumor development and coexistent renal cell carcinoma. *J Urol* 1999;162:40–2.
6. Pavlovich CP, Schmidt LS, Phillips JL. The genetic basis of renal cell carcinoma. *Urol Clin North Am* 2003;30:437–54.
7. Storkel S, Eble JN, Adlakha K, et al. Classification of renal cell carcinoma: Workgroup No. 1. Union Internationale Contre le Cancer (UICC) and the American Joint Committee on Cancer (AJCC). *Cancer (Phila)* 1997;80:987–9.
8. Gnarr JR, Tory K, Weng Y, et al. Mutations of the VHL tumour suppressor gene in renal carcinoma. *Nat Genet* 1994;7:85–90.
9. Kovacs G, Frisch S. Clonal chromosome abnormalities in tumor cells from patients with sporadic renal cell carcinomas. *Cancer Res* 1989;49:651–9.
10. Schmidt L, Duh FM, Chen F, et al. Germline and somatic mutations in the tyrosine kinase domain of the MET proto-oncogene in papillary renal carcinomas. *Nat Genet* 1997;16:68–73.
11. Crotty TB, Lawrence KM, Moertel CA, et al. Cytogenetic analysis of six renal oncocytomas and a chromophobe cell renal carcinoma. Evidence that -Y, -1 may be a characteristic anomaly in renal oncocytomas. *Cancer Genet Cytogenet* 1992;61:61–6.
12. Li E, Bestor TH, Jaenisch R. Targeted mutation of the DNA methyltransferase gene results in embryonic lethality. *Cell* 1992;69:915–26.
13. Jones PA, Baylin SB. The fundamental role of epigenetic events in cancer. *Nat Rev Genet* 2002;3:415–28.
14. Eads CA, Danenberg KD, Kawakami K, et al. MethyLight: a high-throughput assay to measure DNA methylation. *Nucleic Acids Res* 2000;28:E32.
15. Dammann R, Li C, Yoon JH, Chin PL, Bates S, Pfeifer GP. Epigenetic inactivation of a RAS association domain family protein from the lung tumour suppressor locus 3p21.3. *Nat Genet* 2000;25:315–9.
16. Yoon JH, Dammann R, Pfeifer GP. Hypermethylation of the CpG island of the RASSF1A gene in ovarian and renal cell carcinomas. *Int J Cancer* 2001;94:212–7.
17. Dopazo J, Carazo JM. Phylogenetic reconstruction using an unsupervised growing neural network that adopts the topology of a phylogenetic tree. *J Mol Evol* 1997;44:226–33.
18. Virmani AK, Tsou JA, Siegmund KD, et al. Hierarchical clustering of lung cancer cell lines using DNA methylation markers. *Cancer Epidemiol Biomark Prev* 2002;11:291–7.
19. Paz MF, Fraga MF, Avila S, et al. A systematic profile of DNA methylation in human cancer cell lines. *Cancer Res* 2003;63:1114–21.
20. Eads CA, Lord RV, Wickramasinghe K, et al. Epigenetic patterns in the progression of esophageal adenocarcinoma. *Cancer Res* 2001;61:3410–8.
21. Jeronimo C, Usadel H, Henrique R, et al. Quantitation of GSTP1 methylation in non-neoplastic prostatic tissue and organ-confined prostate adenocarcinoma. *J Natl Cancer Inst (Bethesda)* 2001;93:1747–52.
22. Lehmann U, Langer F, Feist H, Glockner S, Hasemeier B, Kreipe H. Quantitative assessment of promoter hypermethylation during breast cancer development. *Am J Pathol* 2002;160:605–12.
23. Morris MR, Hesson LB, Wagner KJ, et al. Multigene methylation analysis of Wilms' tumour and adult renal cell carcinoma. *Oncogene* 2003;22:6794–801.
24. Battagli C, Uzzo RG, Dulaimi E, et al. Promoter hypermethylation of tumor suppressor genes in urine from kidney cancer patients. *Cancer Res* 2003;63:8695–9.
25. Ehrlich M, Jiang G, Fiala E, et al. Hypomethylation and hypermethylation of DNA in Wilms tumors. *Oncogene* 2002;21:6694–702.
26. Yegnasubramanian S, Kowalski J, Gonzalzo ML, et al. Hypermethylation of CpG islands in primary and metastatic human prostate cancer. *Cancer Res* 2004;64:1975–86.
27. Dreijerink K, Braga E, Kuzmin I, et al. The candidate tumor suppressor gene, RASSF1A, from human chromosome 3p21.3 is involved in kidney tumorigenesis. *Proc Natl Acad Sci USA* 2001;98:7504–9.
28. Herman JG, Latif F, Weng Y, et al. Silencing of the VHL tumor-suppressor gene by DNA methylation in renal carcinoma. *Proc Natl Acad Sci USA* 1994;91:9700–4.
29. Kondo K, Yao M, Yoshida M, et al. Comprehensive mutational analysis of the VHL gene in sporadic renal cell carcinoma: relationship to clinicopathological parameters. *Genes Chromosomes Cancer* 2002;34:58–68.
30. Lubinski J, Hadaczek P, Podolski J, et al. Common regions of deletion in chromosome regions 3p12 and 3p14.2 in primary clear cell renal carcinomas. *Cancer Res* 1994;54:3710–3.
31. Yamakawa K, Morita R, Takahashi E, Hori T, Ishikawa J, Nakamura Y. A detailed deletion mapping of the short arm of chromosome 3 in sporadic renal cell carcinoma. *Cancer Res* 1991;51:4707–11.
32. Morrissey C, Martinez A, Zatyka M, et al. Epigenetic inactivation of the RASSF1A 3p21.3 tumor suppressor gene in both clear cell and papillary renal cell carcinoma. *Cancer Res* 2001;61:7277–81.

Clinical Cancer Research

Molecular Profiling and Classification of Sporadic Renal Cell Carcinoma by Quantitative Methylation Analysis

Mark L. Gonzalgo, Srinivasan Yegnasubramanian, Gai Yan, et al.

Clin Cancer Res 2004;10:7276-7283.

Updated version Access the most recent version of this article at:
<http://clincancerres.aacrjournals.org/content/10/21/7276>

Cited articles This article cites 28 articles, 10 of which you can access for free at:
<http://clincancerres.aacrjournals.org/content/10/21/7276.full#ref-list-1>

Citing articles This article has been cited by 4 HighWire-hosted articles. Access the articles at:
<http://clincancerres.aacrjournals.org/content/10/21/7276.full#related-urls>

E-mail alerts [Sign up to receive free email-alerts](#) related to this article or journal.

Reprints and Subscriptions To order reprints of this article or to subscribe to the journal, contact the AACR Publications Department at pubs@aacr.org.

Permissions To request permission to re-use all or part of this article, use this link
<http://clincancerres.aacrjournals.org/content/10/21/7276>.
Click on "Request Permissions" which will take you to the Copyright Clearance Center's (CCC) Rightslink site.